MANSOURA JOURNAL OF Chemistry
Official Journal of Faculty of Science, Mansoura University, Egypt
E-mail: scimag@mans.edu.eg ISSN: 2974-4938

Eco-Friendly Synthesis of Nanocrystalline Hydroxyapatite Bioceramic from a Natural Waste Source: Bovine Bone

Ayda Adel[a] *, Amr M. Abdelghany*[b]*, Magdy Y. Abdelaal*[1a]

[a]*Chemistry Department, Faculty of Science, Mansoura University, Mansoura, 35516, Egypt*

[b]*Spectroscopy Department, Physics Research Institute, National Research Centre, 33 Elbehouth St., Dokki, 123111, Giza, Egypt*

**** Correspondence to:*** *aydaadel2020@gmail.com*

Received:8/9/2025
Accepted:15/9/2025

Abstract: The escalating demand for sustainable biomaterials has driven research into valorizing natural waste sources. This study presents an eco-friendly synthesis route for producing nanocrystalline hydroxyapatite (nHA) from bovine bone waste, a plentiful and underutilized byproduct. The process involved cleaning, drying, and calcining the bone at 1000°C for 4 hours in ambient air, followed by ball milling to produce a fine powder. The synthesized bio ceramic was thoroughly characterized using Fourier Transform Infrared (FTIR) spectroscopy, X-ray diffraction (XRD), transmission electron microscopy (TEM), and scanning electron microscopy coupled with energy-dispersive X-ray spectroscopy (SEM/EDAX). The results confirmed the formation of a highly crystalline, phase-pure hydroxyapatite with a carbonate substitution characteristic of bone-derived apatite. XRD analysis, supported by the Scherrer equation, and TEM imaging revealed a nanocrystalline structure with an average crystallite/particle size of ~30 nm and a spherical morphology. The Ca/P atomic ratio of 1.77, determined by EDAX, was close to the theoretical stoichiometric value for HA. This work demonstrates a simple, green method to transform biological waste into a high value nanocrystalline bioceramic with superior properties, making it a promising candidate for advanced biomedical applications such as bone grafts, implants, and drug delivery systems.

Keywords: Hydroxyapatite; Bovine Bone; Bio ceramic; Nanocrystalline; Eco-friendly Synthesis.

1. Introduction

The escalating demand for advanced biomaterials in orthopedics and dentistry has positioned hydroxyapatite (HA, $Ca_{10}(PO_4)_6(OH)_2$) as a cornerstone of modern bio ceramic research, owing to its exceptional biocompatibility [1], Oste conductivity [2], and chemical resemblance to the inorganic mineral phase of natural bone [3]. While synthetic HA can be produced through various chemical routes, these processes often involve high temperatures, complex procedures, and costly precursors, raising economic and environmental concerns [4, 5]. In parallel, the agricultural industry generates millions of tons of bovine bone waste annually [6], presenting a significant disposal challenge and an underutilized resource. This convergence of needs has catalyzed the exploration of sustainable, eco-friendly synthesis methods to transform this natural waste into high-value medical-grade materials [7, 8]. The conversion of bovine bone into nanocrystalline hydroxyapatite (nHA) represents a paradigm of a circular economy, effectively valorizing a waste product into a sophisticated biomaterial [9]. This approach not only mitigates environmental waste but also capitalizes on the innate, complex architecture and composition of natural bone, which often results in a bio ceramic with superior biological properties compared to its synthetically produced counterparts. However, replicable producing a high purity, nanocrystalline powder with controlled morphology through a simple

calcination process requires precise optimization of parameters such as temperature, atmosphere, and pre-treatment steps [9, 10]. Therefore, this study is dedicated to the development and thorough characterization of an eco-friendly synthesis route for producing nanocrystalline hydroxyapatite Bio ceramic from natural bovine bone waste, analyzing its physicochemical, structural, and morphological properties to assess its potential for biomedical applications.

The pursuit of sustainable biomaterials has driven significant research into deriving hydroxyapatite (HA) from natural bovine bone [11], an abundant and biocompatible waste resource. Previous studies have conclusively established that a calcination process between 800°C and 1000°C effectively removes organic matter and yields a mineral phase primarily composed of carbonated hydroxyapatite, which often demonstrates superior bioactivity due to its trace ion content and resemblance to human bone mineral [12-14]. However, a predominant focus of this existing body of work has been on producing micro-sized HA powders, with less emphasis on the precise control of the calcination parameters to consistently obtain a pure, nanocrystalline structure without excessive grain growth [15]. This gap is critical, as nanocrystalline morphology offers a dramatically increased surface area, which is theorized to significantly enhance bioactivity, desorption rates, and functional properties for advanced applications in drug delivery and nanocomposites [16]. The study of eco-friendly synthesis of nanocrystalline hydroxyapatite bio ceramic from a natural waste source: bovine bone directly addresses this through optimizing a simple thermal process to meticulously control crystal size in the nanoscale regime.

The presented work introduces a precise optimization of a straightforward thermal calcination process to consistently produce a phase- pure, nanocrystalline HA from a natural waste source (bovine bone). While previous studies have often focused on producing micro-sized HA from bone, this research specifically targets and achieves precise control over the nanocrystalline morphology (~30 nm) without the need for complex chemical synthesis or additives. The demonstration of a one-to-one correlation between particle and crystallite size (indicating single-crystal nanoparticles) via combined XRD and TEM analysis is a key finding, revealing a specific recrystallization mechanism that avoids excessive sintering. This work provides a comprehensive green synthesis route that effectively transforms waste into a high-performance nanoceramic, offering a sustainable and economically viable alternative to conventional synthetic methods for advanced biomedical applications.

2. Experimental Techniques

Natural bovine femur bones were sourced from a local slaughterhouse. The bones were thoroughly cleaned to remove adhering flesh, marrow, and other biological residues. This was achieved by repeated boiling in deionized water for several hours, followed by manual scraping. The cleaned bones were then dried in a hot air oven at 120°C for 24 hours to remove moisture. The dried bone samples were crushed into smaller fragments (~2-5 cm) using a mechanical crusher to facilitate further processing.

The cleaned and crushed bone fragments were subjected to a heat treatment process to remove organic constituents and obtain a pure inorganic apatite phase. The samples were placed in a high-temperature alumina crucible and calcined in a programmable muffle furnace. The calcination process was carried out in an ambient air atmosphere at 1000°C with a dwell time of 4 hours at this temperature. The furnace is then switched off and kept cooling naturally to room temperature. The temperature was chosen based on previous studies to ensure complete organic compartment removal while preventing the decomposition of hydroxyapatite.

The calcined white, brittle bone fragments were ground into a fine powder using a high energy planetary Ball Mill Emax (Retsch GmbH, Germany) operating at 1500 rpm for 2 hours. A 1:1 mass ratio of zirconium oxide grinding balls to sample was employed to achieve a nanocrystalline powder. The resulting fine powder was subsequently sieved through a sieve to ensure uniformity and eliminate any large agglomerates.

The X-ray diffraction (XRD) patterns of the prepared powdered sample were collected using

PANalytical X'pert Pro MPD (with wavelength λ = 1.5406 Å, Cu-Kα radiation, and operating voltage 35 kV) in the 2Θ range (5–70°) in a continuous mode. FT-IR spectra measurements were carried out using a Bruker FT-IR spectrometer (Invenio S, Germany). The spectral resolution was 4 cm^{-1}, scan number was 64 within the wavenumber range of 4000–400 cm^{-1} was applied to the collection of ATR spectra. Scanning electron microscopy (QUANTA FEG 250 FE-SEM) was employed to analyze the surfaces of the specimens, their exact structures, crystalline structure, and materials composing the specimens. Images and particle sizes of HA was detected by TEM by using (JEOL JEM-2100, Japan) with 200 kV analytical electron microscope

3. Results and Discussion

3.1. FTIR analysis of synthesized HA

Fourier Transform Infrared (FTIR) spectroscopy was employed to identify the functional groups and chemical bonds present in the calcined bovine bone powder, confirming the formation of hydroxyapatite (HA) and revealing its biomimetic nature Figure (1).

The analysis revealed characteristic absorption bands corresponding to the phosphate (PO_4^{3-}) and hydroxyl (OH^-) groups that define the HA structure. The dominant spectral features were attributed to the vibrational modes of the phosphate tetrahedron: strong asymmetric stretching vibrations (ν_3) of the P–O bonds were observed as broad bands at 1087 and 1026 cm^{-1}, while the symmetric stretching vibration (ν_1) produced a sharp peak at 962 cm^{-1} [17, 18]. Furthermore, the asymmetric bending vibrations (ν_4) of the O–P–O bonds were clearly identified as distinct peaks at 599, 563, and 473 cm^{-1} [19].

The presence of the hydroxyl group was confirmed by a sharp band at 630 cm^{-1}, corresponding to the liberation mode of the OH^- ion, and a broad, weak band observed at 3550 cm^{-1}, associated with the O–H stretching vibration [18-21]. The sharpness and well-defined positions of these peaks are indicative of a highly crystalline HA phase. Additionally, the spectrum exhibited low-intensity bands at 1453 and 873 cm^{-1}, which are characteristic of carbonate (CO_3^{2-}) ions incorporated into the apatite lattice through B-type substitution, a hallmark of bone-derived hydroxyapatite that enhances its biological compatibility. Obtained results can be summarized as shown in Table (1).

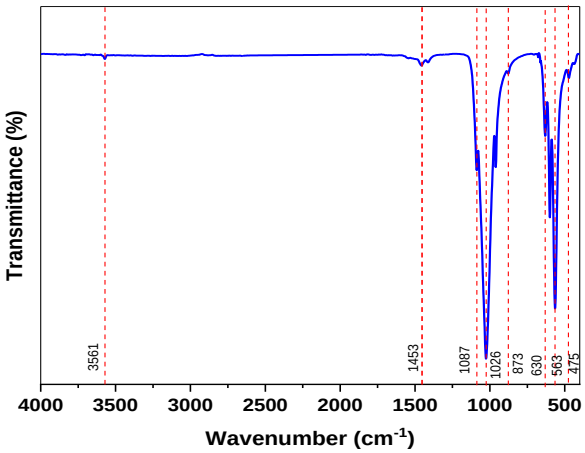

Figure (1) FTIR spectra of the synthesized HA

Table (1) FTIR band position and assignment of synthesized HA

Wavenumber	Assignment	Ref.
473, 563, 599	Bending $(PO_4)^{3-}$	17, 18, 19
630	Bending $(OH)^-$	17
961	Symmetric Stretching $(PO_4)^{3-}$	17, 18, 19
1088, and 1025	Asymmetric Stretching $(PO_4)^{3-}$	19, 20
1412, 1457, 877	$(CO_3)^{2-}$	19, 20
3566	$(OH)^-$	17-21

3.2. X-ray diffraction (XRD)

The X-ray diffraction (XRD) analysis of the bovine bone calcined at 1000°C, presented in Figure (2), conclusively identifies the resultant material as highly crystalline, phase-pure hydroxyapatite (HA, $Ca_{10}(PO_4)_6(OH)_2$). The diffraction pattern exhibits all characteristic peaks of stoichiometric HA, showing excellent agreement with the standard JCPDS card #09-0432. The most intense peak, a defining feature of the HA crystal structure, is observed as a doublet centered at approximately 31.8° 2θ, which corresponds to the overlapping reflections from the (211) and (112) crystallographic planes. This high-intensity peak, along with other strong and well-defined reflections such as the (002) plane at 25.9° and the (300) plane at 32.9°, confirms a high degree of crystallinity and the absence of secondary phases like tricalcium phosphate (TCP) or calcium oxide [19-22]. The successful formation of pure HA at this temperature is

attributed to the complete combustion of the organic matrix and the subsequent thermal decomposition and recrystallization of the native bone mineral, which eliminates fewer stable phases and promotes crystal growth. The precise match between the synthesized material's diffraction pattern and the standard confirms that calcination of bovine bone at 1000°C is an effective method for producing a biomaterial with a chemical and structural composition nearly identical to the mineral component of human bone, making it an excellent candidate for biomedical applications such as bone grafts and implants where bioactivity and osteoconductivity are paramount [22].

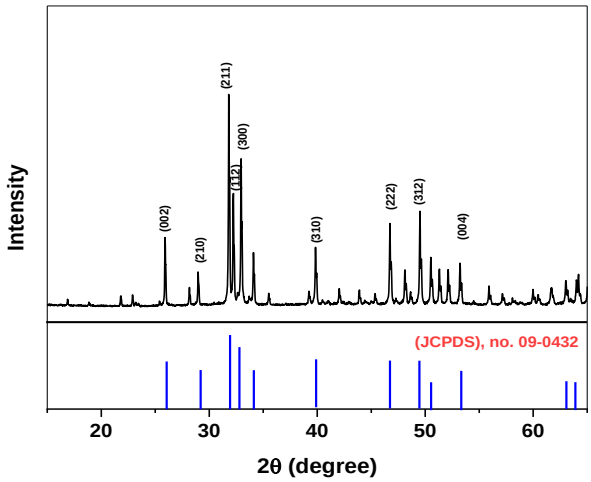

Figure (2) XRD pattern of the studied HA

To quantify the crystallite size of the synthesized hydroxyapatite, the Scherrer equation was employed. This equation relates the broadening of a diffraction peak to the size of the crystallites, under the assumption that size effects are the primary contributor to peak broadening, as opposed to micro strain or instrumental factors. The analysis was applied to the most intense and well-defined peak, the (211)/ (112) doublet. The Scherrer equation is given by [23-25]:

$D = (K\lambda) / (\beta \cos\theta)$

Where:

D is the average crystallite size (in nm),

K is the dimensionless shape factor, often taken as 0.9 for a spherical crystal with cubic symmetry,

λ is the wavelength of the X-ray radiation (for Cu-Kα, λ = 0.15406 nm),

β is the full width at half maximum (FWHM) of the diffraction peak in radians, after correcting for instrumental broadening,

θ is the Bragg angle (half of the 2θ peak position).

The measured FWHM (β) for the (211) peak at $2\theta \approx 31.8°$ was found to be 0.00297 radians after necessary instrumental broadening correction. Using the values K = 0.9 and λ = 0.15406 nm, and with θ = 15.9°, the calculated average crystallite size was determined to be approximately 30 nm. This result confirms that the calcination process at 1000°C successfully produced a nano-crystalline hydroxyapatite powder. The nanoscale dimension of the crystallites is a critical attribute, as it directly influences the material's surface area, solubility, and biological performance, typically enhancing its bioactivity and Oste conductivity potential compared to co-grained materials.

3.3. Transmission electron Microscope

Figure (3) presents the transmission electron microscopy (TEM) image of the synthesized hydroxyapatite (HA) alongside its corresponding particle size distribution histogram. The micrograph unequivocally reveals that the powder consists of nanoparticles with a nearly spherical morphology. The histogram, constructed from measuring a statistically significant number of particles, provides a quantitative assessment, confirming that the average particle size lies within the range of 30 to 35 nanometers. This observation indicates a relatively narrow and homogeneous size distribution, which is a crucial parameter for ensuring consistent biological and mechanical properties in biomedical applications.

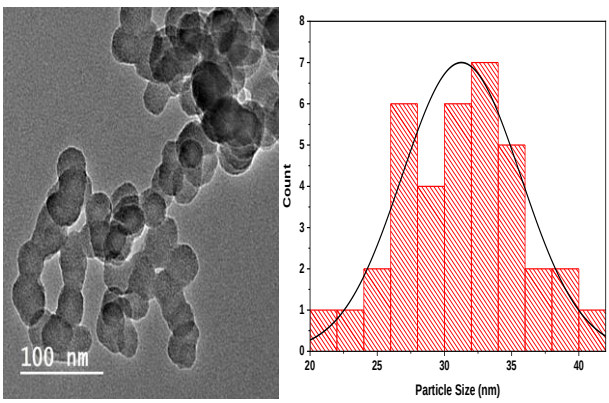

Figure (3) TEM analysis of the studied HA with histogram

The TEM results exhibit a remarkable and consistent correlation with the data obtained from X-ray diffraction (XRD) analysis. The XRD analysis, using the Scherrer equation on the broadening of the (211) peak, calculated an average crystallite size of approximately 30 nm. The close agreement between the TEM particle size (30-35 nm) and the XRD crystallite size (~30 nm) leads to a critical conclusion: each individual nanoparticle observed in the TEM image is, in fact, a single crystal [26, 27].

This one-to-one relationship between particle and crystallite size signifies a high degree of crystallinity and a specific formation mechanism. It indicates that the calcination process at 1000°C did not lead to extensive sintering or fusion of multiple primary crystals into larger, polycrystalline granules. Instead, the heat treatment effectively removed the organic matrix and allowed the native bone mineral to recrystallize into discrete, well-defined nanocrystals. The nearly spherical shape further suggests a low-energy equilibrium form and is advantageous for applications like bio-inks or composite materials where flowability and packing density are important [28].

Therefore, the TEM analysis provides direct visual evidence that strongly supports the XRD findings. Together, these techniques paint a comprehensive picture of the synthesized material: a phase-pure hydroxyapatite composed of discrete, single-crystal nanoparticles with a spherical morphology and an average size of ~30 nm**.** This nanoscale, highly crystalline structure is paramount as it mimics the natural nano-architecture of bone mineral, promising enhanced surface reactivity, improved biodegradability, and superior bioactivity for bone tissue engineering applications.

3.4. Scanning electron microscope supported energy dispersive X-ray (SEM/EDAX)

The morphology of the as-synthesized hydroxyapatite (HA) nanoparticles was investigated using scanning electron microscopy (SEM), as presented in Figure (4a). The micrographs reveal that the nanoparticles are highly agglomerated, forming larger clusters. This agglomeration is a common phenomenon in nanoscale powders and can be attributed to high surface energy driving particle cohesion, potentially through mechanisms such as Ostwald ripening [29, 30]. Despite the agglomeration, the primary particles are discernible and exhibit a spherical shape, which is consistent with the morphological findings from TEM analysis. Furthermore, the SEM image shows a highly porous surface morphology, characterized by numerous voids and pores. This is a direct result of the calcination process, where thermal decomposition and combustion of the organic collagen matrix within the raw bovine bone leave behind a porous inorganic HA structure. This stands in stark contrast to the dense, smooth micro-surface typical of unprocessed raw bone particles. To confirm the chemical composition, energy-dispersive X-ray (EDX) spectroscopy was performed, with the spectrum shown in Figure (4b).

The analysis detected primarily calcium (Ca) and phosphorus (P), along with oxygen (O), confirming the expected elemental constituents of HA. The atomic ratio of Ca to P, a critical metric for identifying stoichiometric hydroxyapatite, was calculated from the weight percentages provided in Table (2). The calculated Ca/P ratio of 1.77 (from Ca: 21.04 wt.% / P: 12.44 wt.%) is very close to the theoretical stoichiometric value of 1.69, confirming the successful synthesis of a near-pure hydroxyapatite phase with minimal ionic substitution.

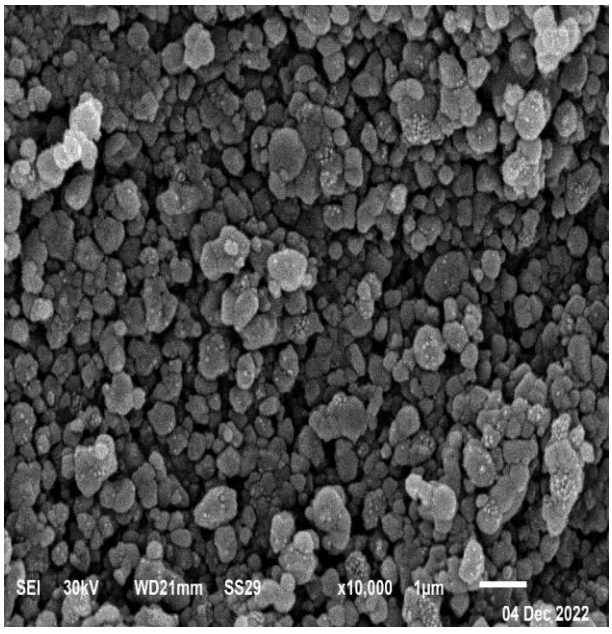

(a)

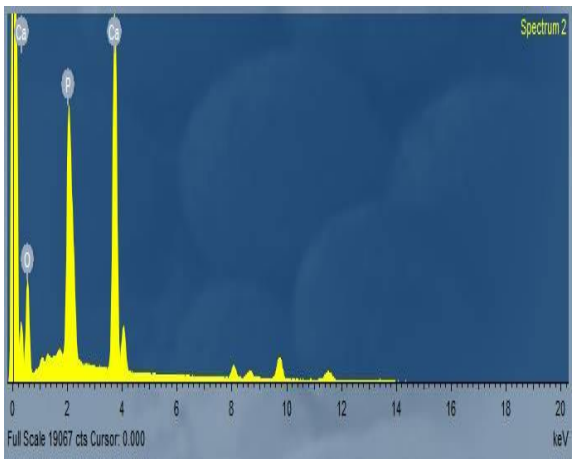

(b)

Figure (4 a,b): SEM and EDAX analysis of the studied HA-NPs.

Table (2) EDAX analysis results of Studied HA

	Weight%	**Atomic%**
O K	67.93	82.82
P K	12.44	6.24
Ca K	21.04	10.24

4. Conclusion

This study successfully established a simple and eco-friendly method for synthesizing high purity nanocrystalline hydroxyapatite (nHA) from natural bovine bone waste. Comprehensive characterization confirmed that calcination at 1000°C effectively removed the organic matrix and yielded a highly crystalline, single-phase hydroxyapatite powder. The presence of carbonate ions in the apatite structure, a hallmark of bone-derived HA, was identified, enhancing its biomimetic properties. Crucially, the combination of XRD analysis and TEM imaging demonstrated that the synthesized HA consists of discrete, single-crystal nanoparticles with a nearly spherical morphology and a narrow size distribution averaging ~30 nm. The measured Ca/P ratio further confirmed the formation of a near-stoichiometric composition. The successful conversion of an abundant agricultural waste into a nanoscale biomaterial with superior attributes—such as high surface area and expected enhanced bioactivity—highlights the significant potential of this material for use in demanding biomedical applications, including bone tissue engineering, implant coatings, and nanocomposites, while promoting a circular economy.

References

1. Jaiswal, S., Dubey, A., & Lahiri, D. (2019). In vitro biodegradation and biocompatibility of Mg–HA-based composites for orthopaedic applications: a review. *Journal of the Indian Institute of Science*, **99(3)**, 303-327.
2. Kozuma, W., Kon, K., Kawakami, S., Bobothike, A., Iijima, H., Shiota, M., & Kasugai, S. (2019). Osteoconductive potential of a hydroxyapatite fiber material with magnesium: In vitro and in vivo studies. *Dental Materials Journal*, ***38*(5)**, 771-778.
3. Nicholson, J. W. (2020). The chemistry of medical and dental materials (Vol. **7**). Royal Society of Chemistry.
4. Enax, J., & Epple, M. (2018). Synthetic hydroxyapatite as a biomimetic oral care agent. Oral health & preventive *dentistry*, **16(1).**
5. Zhou, J., Zhang, X., Chen, J., Zeng, S., & De Groot, K. (1993). High temperature characteristics of synthetic hydroxyapatite. *Journal of materials science: materials in medicine*, **4(1)**, 83-85.
6. Hart, A., Ebiundu, K., Peretomode, E., Onyeaka, H., Nwabor, O. F., & Obileke, K. (2022). Value-added materials recovered from waste bone biomass: technologies and applications. RSC advances, **12(34)**, 22302-22330.
7. Andrade, F. A. C., de Oliveira Vercik, L. C., Monteiro, F. J., & da Silva Rigo, E. C. (2016). Preparation, characterization and antibacterial properties of silver nanoparticles–hydroxyapatite composites by a simple and eco-friendly method. Ceramics international, **42(2)**, 2271-2280.
8. Gurawalia, P., Majumder, S., Srivastava, C. M., Charak, S., & Shandilya, M. (2024). Green Synthesis of Hydroxyapatite Nanoparticles: Sustainable Approaches for Biomedical Advancements. In Eco-Materials and Green Energy for a Sustainable Future (pp. 95-117). CRC Press.
9. Oluremi, D. (2025). Sustainability and Eco-friendly Sources of Hydroxyapatite for Biomedical Use.

10. Alaneme, K. K., Oke, S. R., Fagbayi, S. B., Alabi, O. O., Ojo, O. M., Kareem, S. A., & Folorunso, D. O. (2025). Synthesis and structural analysis of calcined poultry manure for hydroxyapatite development. Next Sustainability, 5, 100079.
11. Razak, M., & Gamagedara, T. P. (2025). Green synthesis and characterization of hydroxyapatite nanoparticles using cow dung for biomedical applications. *Ceylon Journal of Science*, **54(3).**
12. Rai, D., Mahanty, A., Kumar, R., Shikha, D., Anand, S., & Sinha, S. K. (2025). Effects of Sintering Temperature on the Microstructure, Microhardness, and Corrosion Resistance of Hydroxyapatite. *Journal of Materials Engineering and Performance*, 1-9.
13. Tran, D. L., Ta, Q. T. H., Tran, M. H., Nguyen, T. M. H., Le, N. T. T. T., Hong, A. P. N., & Nguyen, D. H. (2025). Optimized synthesis of biphasic calcium phosphate: enhancing bone regeneration with a tailored β-tricalcium phosphate/hydroxyapatite ratio. Biomaterials Science, **13(4)**, 969-979.
14. Mortada, W. I., Kenawy, I. M., Abdelghany, A. M., Ismail, A. M., Donia, A. F., & Nabieh, K. A. (2015). Determination of Cu2+, Zn2+ and Pb2+ in biological and food samples by FAAS after preconcentration with hydroxyapatite nanorods originated from eggshell. Materials Science and Engineering: C, **52**, 288-296.
15. Hababi, E., Harabi, A., Foughali, L., Chehlatt, S., Zouai, S., & Mezahi, F. (2015). Grain growth in sintered natural hydroxyapatite. Acta Physica Polonica A, **127(4)**, 1161-1163.
16. Mondal, S., Dorozhkin, S. V., & Pal, U. (2018). Recent progress on fabrication and drug delivery applications of nanostructured hydroxyapatite. Wiley Interdisciplinary Reviews: Nanomedicine and Nanobiotechnology, **10(4),** e1504.
17. Thamizharasi, V., Venda, I., Indira, J., Selvakumaran, M., Kubaib, A., Yassin, M. T., & Prakash, V. C. A. (2025). Tuning the Growth of HAP Crystal with GA: FTIR, XRD, Morphological Characterization, in-vitro Proliferation Studies and Computational Evaluation. *Journal of Molecular Structure*, 143165.
18. Hossain, M. S., & Ahmed, S. (2023). FTIR spectrum analysis to predict the crystalline and amorphous phases of hydroxyapatite: a comparison of vibrational motion to reflection. RSC advances, **13(21),** 14625-14630.
19. Shaltout, A. A., Allam, M. A., & Moharram, M. A. (2011). FTIR spectroscopic, thermal and XRD characterization of hydroxyapatite from new natural sources. *Spectrochimica* Acta Part A: Molecular and Biomolecular Spectroscopy, **83(1),** 56-60.
20. Ślósarczyk, A., Paszkiewicz, Z., & Paluszkiewicz, C. (2005). FTIR and XRD evaluation of carbonated hydroxyapatite powders synthesized by wet methods. *Journal of Molecular Structure*, **744**, 657-661.
21. Reyes-Gasga, J., Martínez-Piñeiro, E. L., Rodríguez-Álvarez, G., Tiznado-Orozco, G. E., García-García, R., & Brès, E. F. (2013). XRD and FTIR crystallinity indices in sound human tooth enamel and synthetic hydroxyapatite. Materials Science and Engineering: C, **33(8),** 4568-4574.
22. Okur, H. E. (2025). Rietveld refinement-based structural analysis of biogenic hydroxyapatite and its PVA composite for dye removal. Materials Today Communications, **43**, 111723.
23. Abdelbaky, M., Abdelghany, A. M., Oraby, A. H., & Rashad, M. M. (2025). Ultraviolet-stimulated photocatalysis of crystal violet using (Gd (2-x) La (x) Zr (2-x) Sn (x) O7) pyrochlore nanoparticles. Applied Water Science, **15(7),** 168.
24. Ahmed, E., Aly, H. M., Abdelghany, A. M., & Ismail, A. A. (2025). Structure and radiation shielding attitude of hexa-structured borosilicate glasses containing zinc oxide. Applied Physics A, **131(5),** 1-10.
25. Muniz, F. T. L., Miranda, M. R., Morilla dos Santos, C., & Sasaki, J. M. (2016).

The Scherrer equation and the dynamical theory of X-ray diffraction. Foundations of Crystallography, **72(3)**, 385-390.
26. Nasiri-Tabrizi, B., Honarmandi, P., Ebrahimi-Kahrizsangi, R., & Honarmandi, P. (2009). Synthesis of nanosize single-crystal hydroxyapatite via mechanochemical method. Materials Letters, **63(5),** 543-546.
27. Sun, Y., Guo, G., Wang, Z., & Guo, H. (2006). Synthesis of single-crystal HAP nanorods. Ceramics International, **32(8)**, 951-954.
28. Redey, S. A., Nardin, M., Bernache–Assolant, D., Rey, C., Delannoy, P., Sedel, L., & Marie, P. J. (2000). Behavior of human osteoblastic cells on stoichiometric hydroxyapatite and type A carbonate apatite: role of surface energy. *Journal of Biomedical Materials Research: An Official Journal of The Society for Biomaterials, The Japanese Society for Biomaterials, and The Australian Society for Biomaterials and the Korean Society for Biomaterials*, **50(3),** 353-364.
29. Wei, M., Ruys, A. J., Milthorpe, B. K., & Sorrell, C. C. (1999). Solution ripening of hydroxyapatite nanoparticles: effects on electrophoretic deposition. *Journal of Biomedical Materials Research: An Official Journal of The Society for Biomaterials, The Japanese Society for Biomaterials, and The Australian Society for Biomaterials*, **45(1),** 11-19.
30. Goldberg, M. A., Antonova, O. S., Donskaya, N. O., Fomin, A. S., Murzakhanov, F. F., Gafurov, M. R., ... & Komlev, V. S. (2023). Effects of various ripening media on the mesoporous structure and morphology of hydroxyapatite powders. Nanomaterials, **13(3),** 418.